



REGULAR ARTICLE

A Y-Shaped Patches Massive MIMO Antenna for Performance Measures in 6G Application

Kumutha Duraisamy^{1,*}, P. Geetha², P. Gobi³, K. Arun¹, P. Latha⁴, Manjunathan Alagarsamy⁵

¹ Department of CSE, Jeppiaar Institute of Technology, Kunnam, Sriperumudur, 631604 Chennai, India

² Department of Electronics and Communication Engineering, Karpaga Vinayaga College of Engineering and Technology, 603308 Chennai, India

³ Department of ECE, Jeppiaar Institute of Technology, Kunnam, Sriperumudur, 631604 Chennai, India

⁴ Department of IT, Panimalar Engineering College, Chennai, India

⁵ Department of ECE, K. Ramakrishnan College of Technology, Trichy, India

(Received 12 April 2025; revised manuscript received 18 August 2025; published online 29 August 2025)

In the current era, the fifth generation (5G) determines the latency as 1 ms with high data speed for mobile communication networks. During the investigation of using the 5G networks, the power efficiency was higher, and spectrum usage was increased in the coverage of signal in the Massive 2-2 MIMO (Multiple Input and Multiple Output) Antenna. Hence the Sixth generation (6G) is introduced which will support the Massive 2-2 MIMO for 10 times better than the 5G in the mobile communication system. 6G provides 1 μ s with less power consumption through the efficiency with equal frequency in the design of Massive 2-2 MIMO Antenna. In wireless communication networks, a protocol such as Message Queuing Telemetry Transport (MQTT) is also proposed to use efficient Bandwidth and avoid delay while transmitting high-speed data rate for multiple users. MQTT supports liberating from the security issues during the several transmissions in the Massive MIMO System. A massive 2-2 MIMO antenna is designed for 10 GHz frequency to reduce inter-symbol interference (ISI), resulting in 88 % efficiency. The Y-shaped patches are modeled with a radius of 8.5 mm at the top layer for the two elements. The dimension is grounded with 8.5 mm \times 65 mm \times 2 mm to provide better improvement of the system. The proposed system used the operating frequency ranging from 2.7 GHz to 15.8 GHz with 15 dB return loss and isolation of 12 dB for the MQTT protocol with Massive MIMO antenna. The High-frequency Simulator (HFSS) provides a relative permittivity of 2.7, isolation of 13 dB, and directivity of 5. Also, the gain is achieved for 6.7 dB with an efficiency of 88 % compared to the conventional method.

Keywords: 6G, Massive 2-2 MIMO, HFSS, MQTT, ISI, Mobile communication.

DOI: [10.21272/jnep.17\(4\).04023](https://doi.org/10.21272/jnep.17(4).04023)

PACS number: 84.40.Ba

1. INTRODUCTION

Ref. [1] describes the design of an integrated antenna with dimensions of 30 \times 10 \times 1.6 mm³, optimized for operation in many communications, especially Wi-I and sub-6 GHz frequencies. The 3.5 GHz and 5- GHz range make this antenna suitable for many practical applications. The paper also demonstrates an effective technique for reducing coupling, which is to create a negative ground pattern (NGR) of the antenna points by combining two intersections in a field. By using this technique, the coupling at 2.46 GHz and 3.47 GHz is decreased from 6.5 dB and 9 dB to 26 dB and 13 dB, correspondingly [2-5]. For Internet access applications, this paper suggests a compact, minimal coupling, broadband 4 \times 4 MIMO antenna design. The antenna is made up of four separate antenna components, each measuring 15.2 \times 3.5 \times 0.8 mm³ and having multi-branch architectures. The multiple-mode resonance technique is used to accomplish the broadband features, and neighbouring antenna components are placed orthogonally to guarantee that their primary radiation directions lead to distinct locations.

For 5G portable terminals, an eight-port antenna's array is suggested in order to facilitate multiple-input multiple-output (MIMO) functions. The printed circuit board (PCB), measuring 150 \times 75 mm², has two components at each of the corners of the arrangement. Different types of radiation along with linear in shape duality polarization are displayed by the apertures and their corresponding radiating components. The antenna efficiently covers the uppermost C-band frequency that ranges from 3.3 GHz to 4.2 GHz for 5G n77 and n78 bands in frequency range 1 (FR1), with a bandwidth surpassing 1000 MHz, from 3 to 4.2 GHz [6-8]. Spatial wave decoupling over the tri-band is made possible by the Archimedean helical metasurface. A small antenna is produced by combining superficial waves with space wavelength decoupling methods. The predicted data and the actual findings agree quite well. In particular, the observed results demonstrate isolation gains of 3.5 dB, 36.47 dB, and 6.42 dB for the frequency bands 3.45-3.55 GHz, 5.7-5.9 GHz, and 6.75-7 GHz, correspondingly, with an approximate reflection coefficient of -10 dB [9]. 75 % of the electromagnetic spectrum will pass through

* Correspondence e-mail: skvijaykumu@gmail.com



the antenna inside its operational frequency band thanks to mobile device antennas' functioning bandwidth of -6 dB. Even though other high-isolation 5G wireless terminal antennas were successfully produced in previous research, which are very limited dual-band wideband MIMO antenna configurations that they can be utilized with smartphone systems. For example, [10] describes a slot-based eight-antenna array for metal-frame telephones.

The structure of this document is as follows: The detailed introduction and its literature survey is explained in detail in section 2. The analysis and its evaluation of the MIMO antenna's design concepts, procedure, and decoupling mechanism is covered in detail in Section 3. Antenna performance, including total gain patterns, efficacy, and ECC, is analyzed in Section 4 by contrasting antennas with and without decoupling structures. The design procedure, techniques, and outcomes of the MIMO antenna created in this paper are compiled in Section 5.

2. LITERATURE REVIEW

Considering the widest variety of challenging applications, antenna patch networks are utilized in the most straightforward manner possible [11]. This section covers the scientific investigation of numerous articles on microstrip patch antennas. For future 5G mobile applications, this article [12] proposes a cellular broadband elliptical-shaped slotted antenna. This study describes several ideas for rectangular microstrip antennas [10]. All of these antennas function at 28 GHz, it is among the frequently used wavelengths communication in 5G. This study's findings [13] concentrated on using a broad range of microstrip antenna designs. A number of important factors, like as gain, resonant frequency, bandwidth, return loss, as well as voltage standing wave ratio (VSWR), can be employed to evaluate the performance of an antenna.

A return loss below -10 dB is regarded as an exceptional value. The range of VSWR values that are considered is 1-2. A state-of-the-art software program called CST Microwave Studio lets users design and test a large range of antennas, filters, and other gadgets.

A high-gain linear 1×4 antenna array having a circle-shaped slotted patch for use in 5G communication applications is discussed in the paper [14]. The suggested antenna, designed for a frequency of 28 GHz, when adjusted to resonance, can support TM₁₁ as a fundamental mode. The suggested antenna's concept has been verified by characterizing the antenna prototype using an anechoic chamber and vector network analyzers (VNA).

In this work, an antenna with a microstrip patch is employed as a communication device [15] and is investigated for increased frequency one-band as well as dual-band transmission. A square-slotted microstrip patch antenna for mm Wave wireless transmission with a resonance wavelength of 37 GHz is presented in this paper [16]. This work designs a 1×2 array microstrip rectangular patched antenna having the two components [17, 18]. The antenna has a frequency of 3.5 GHz, an actual patch size of 19.5 by 26.5 millimeters, along with an array size of 1×2 . A computational model operating at 3.5 GHz is employed

to build the antenna's design; copper is utilized for the patch materials and flame-resistant (FR) 4 (which in turn has a permanent of 4.3) is used for the substrate. 3.5 GHz is the frequency at which the simulation runs.

3. ANTENNA DESIGN AND MQTT PROTOCOL

Integrating MQTT (message queuing telemetry transport) with a massive MIMO (multiple input, multiple output) antenna system offers a unique set of opportunities and challenges, particularly for communication systems that rely on wireless networks.

Enhanced Signal Quality: Massive MIMO can develop the signal-to-noise ratio (SNR) in wireless communication. With a better SNR, the MQTT messages can be delivered with higher reliability and reduced packet loss, which is crucial for applications that rely on continuous and timely data transmission.

Lower Latency: One of the key benefits of Massive MIMO is its ability to reduce latency by directing signals efficiently to the intended receivers. This can result in faster MQTT message delivery times, which is critical for applications requiring near real-time data.

Increased Capacity: MQTT systems often serve environments with many connected devices. Massive MIMO can handle more simultaneous connections by spatially separating users or devices through beamforming, thus reducing congestion and improving the overall scalability of MQTT-based systems.

Energy Efficiency: With beamforming, Massive MIMO can focus energy in specific directions rather than broadcasting signals widely. This can reduce the overall energy consumption, which benefits both the base stations and the end devices (IoT devices) running MQTT clients.

3.1 Geometry

An antenna for ultra wide band operations is suggested in this study. This includes a faulty ground positioned beneath the substrate and a 50 Ω microstrip feed line. Typically, a defective ground plane serves as an electrical barrier in an antenna, which is also an essential part of the feeding mechanism and radiator. Additionally, this modifies the output radiation pattern and input properties. However, in this case, the defective ground's primary goals are to improve bandwidth and change the current distribution. These are employed to attain an electromagnetic pattern that eliminates ripples and ultra-wideband functioning, and omnidirectional coverage. The FR-4 substrate has the rectangle copper placed on it. The ultrawide band monopole antenna measures 1.72 mm by 3 mm by 0.08 mm.

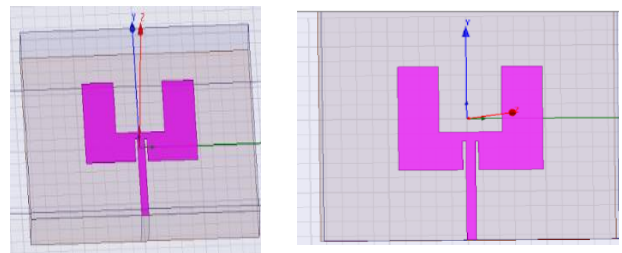


Fig. 1 – (a) and (b) shows the proposed radiator's front and rear views

3.2 Design Procedure

The CST Microwave Studio Software (MWS) is utilized to model and simulation of the antenna parameter design. The Y-shaped patch antenna in Fig. 1a serves as the basis for the modeling. It has a $50\ \Omega$ microstrip feedline with dimensions of $L = 16\text{ mm}$ and $W = 3.13\text{ mm}$, as well as two opposing lines that create a dipole with dimensions of $L_d = 8.5\text{ mm}$ and $W_d = 1.07\text{ mm}$ and an inclination of 57° , which yields the letter Y. The arrangement of the electromagnetic field in a microstrip construction is shown in Figure 2.

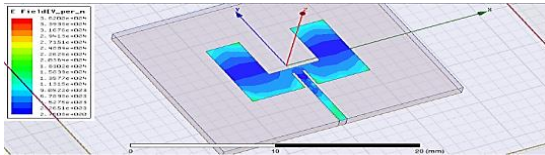


Fig. 2 – Electromagnetic field distribution in a microstrip structure

Two stubs of varying lengths are also present in parallel; one is of $S_1 = 3.5\text{ mm}$ and the other is of $S_2 = 5.5\text{ mm}$. The two lines of the dipole are separated by a 12-mm-long slit in the middle, which is there to improve signal transmission. Two more 70° slanted stubs at the base of the structure, measuring 3 mm and 1 mm in length (L_o) and width (W_o), respectively, aid the top stub to provide a pretty broad bandwidth across all frequencies. Figure 3 represents the 3D Electric field distribution in a planar resonator structure.

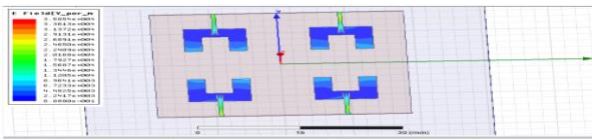


Fig. 3 – 3D electric field distribution in a planar resonator structure

With a permeability of $\epsilon_r = 4.4$ and a loss tangent of $\delta = 0.02$, this design is installed on a FR-4 dielectric substrate. Its dimensions are $26 \times 18 \times 1.6\text{ mm}^3$, which is undoubtedly little, but it still produces good results. A ground plane, seen in Fig. 1b, sits behind this structure. Its width is equal to that of the substrate, and its length (G) is 11.78 mm. This value was tuned using the CST Microwave Studio program, yielding favorable outcomes. Figure 4 represents the electric field distribution in a planar microstrip resonator.

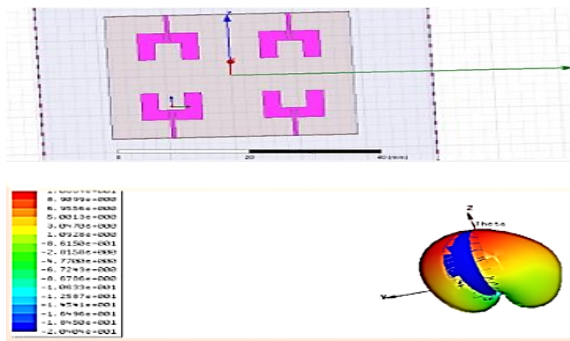


Fig. 4 – Electric field distribution in a planar microstrip resonator

4. RESULTS AND ITS DEISCUSSION

Based on the final outcomes of the simulation, the parameter was found to be accurate. The optimal base value for wireless or mobile technology is -10 dB . To function at the required frequency, the antenna is modified. Figure 4 illustrates its frequency of operation, which is 28 GHz. It was discovered that the return loss at this frequency was -38.348 dB . The S11 parameter describes the proposed antenna's return loss. The return loss at -10 dB is -38.348 dB , as shown in Figure 4. This is an extremely high value which makes it a perfect choice for 5G applications.

Figure 4 displays the antenna's bandwidth, which is 3.464 GHz, between 26.327 GHz and 29.791 GHz. Increased bandwidth is essential for 5G applications. The bandwidth indicated in this effort is ideal for these uses. Because it indicates how effectively the transmission line's impedance is matched, VSWR is a crucial metric for evaluating an antenna's performance.

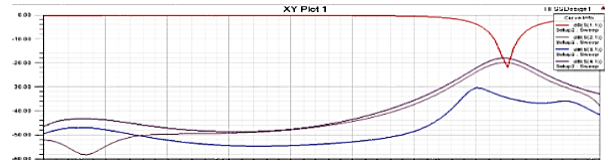


Fig. 5 – Return loss vs frequency of the antenna

For improved performance, the VSWR's bandwidth should be near 1. The VSWR value in Figure 5 is 1.024485, which is extremely near to the minimal range of 1.

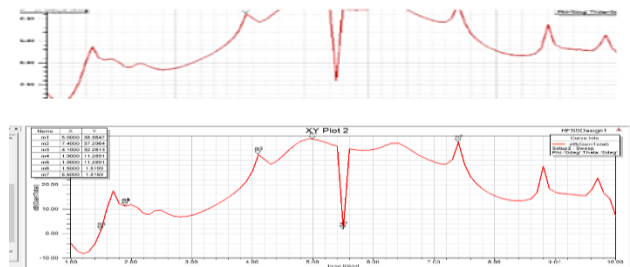


Fig. 6 – VSWR versus the microstrip patch antenna's frequency

The H field, E field, and surface current of the antenna were measured and shown in Figure 6-8. An applied electromagnetic field is the source of the surface current, which is a genuine electric current. Since the E -field is a vector quantity, each point in space has both a magnitude and a direction. Fringe fields have a major impact on a microstrip antenna's performance. With microstrip antennas, there is no electric field at the center of the patch. The radiation is caused by the fringing field that exists between the ground plane and the patch's edge. The antenna's magnetic strength is represented by the H Field.

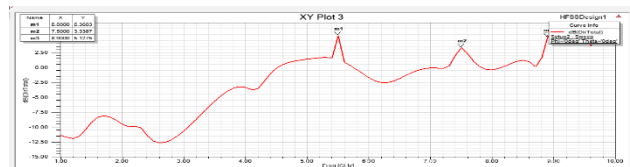


Fig. 7a – Radiation performance – Gain

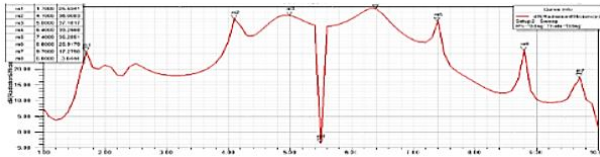


Fig. 7b – Radiation performance – Efficiency

Since it illustrates an antenna's overall performance, the radiation pattern is a crucial component. The microstrip patch antenna's 3D radiation pattern is displayed in Figure 9. According to the figure, 5G technology is highly effective with a gain of 8.2 dBi and a radiation efficacy of 77 %. Furthermore, as shown in Figure 10, the side-lobe level, angular breadth (3 dB), and main-lobe direction are 11.0, 72.5, and -13.8 degrees, correspondingly.

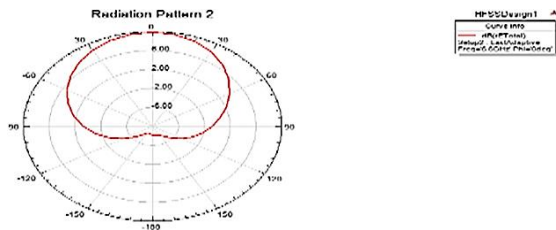


Fig. 8 – The proposed antenna's (a) 10 GHz radiation pattern

It causes an impedance mismatch as it propagates into the antenna, which is what causes power consumption. Consistent data transfer, low power consumption, and less heating are the outcomes of optimal design. The maximum amount of power delivered to the load from the source is made possible by a desired low VSWR, which is achieved when the impedance is matched. The investigated antenna exhibits a smaller return loss when compared to earlier studies. To improve the examined antenna's performance in terms of gain and bandwidth, every

antenna parameter has been adjusted. The bandwidth is larger than that of the antennas listed in [17, 18], as demonstrates.

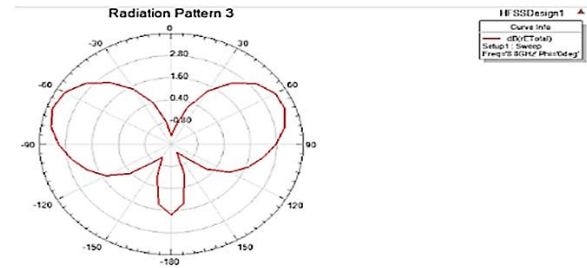


Fig. 9 – The proposed antenna's observed and modeled radiation pattern (a) at 8.8 GHz

When compared to previously published efforts, the developed microstrip patch antenna generally performs remarkably well.

5. CONCLUSION

A small microstrip patch antenna is being researched for 6G technology to achieve high gain resonance at 30.08 GHz. In terms of return losses and VSWR, the Y-shaped dipole patch antenna via stub along with slot provided us with acceptable results. Its 78.8 % bandwidth, which spans the frequencies of 3 GHz to 6.9 GHz, enables it to be used in ultra-wide band applications and meets the FCC report's standards. Transmission losses are quite minimal with the suggested antenna. In addition, the transmission gain reaches 2.87 dBi at 6.5 GHz, which is reasonable for this kind of antenna. From a variety of angles, this antenna can be made better by enhancing its design as much as feasible, selecting other dielectric materials, or improving the feedline to boost bandwidth, reduce reflection, and boost gain.

REFERENCES

- Hehe Yu, et al., *Electronics* **13**, 3585 (2024).
- Chang-Keng Lin, Ding-Bing Lin, Han-Chang Lin, Chang-Ching Lin., *Sensors* **24**, 5495 (2024).
- Y. Hu, Y. Wang, L. Zhang, M. Li, *Micromachines* **15**, 850 (2024).
- Parveez Shariff Bhadravathi Ghouse, et al., *Micromachines* **15**, 729 (2024).
- Asad Ali Khan, et al., *Electronics* **13**, 2196 (2024).
- Guangpu Tang, et al., *Electronics* **13**, 2146 (2024).
- Chong-Zhi Han, et al., *Micromachines* **15**, 705 (2024).
- Kumutha Duraisamy, Tanvir Islam, et al., *J. Nano-Electron. Phys.* **15** No 6, 06029 (2023).
- M. Jeyabharathi, D. Kumutha, et al., *J. Nano-Electron. Phys.* **16** No 4, 04006 (2024).
- D. Kumutha, R. Delshi Howsalya Devi, et al., *J. Nano-Electron. Phys.* **16** No 3, 03007 (2024).
- D. Kumutha, R. Delshi Howsalya Devi, et al., *J. Nano-Electron. Phys.* **16** No 4, 04003 (2024).
- M. Jeyabharathi, D. Kumutha, et al., *J. Nano-Electron. Phys.* **16** No 3, 03008 (2024).
- D. Kumutha, T. Islam, et al., *J. Nano-Electron. Phys.* **16** No 3, 03010 (2024).
- S. Usha, P. Geetha, et al., *J. Nano-Electron. Phys.* **15** No 3, 03009 (2023).
- El Arrouch Tarik, Najiba El Amrani El Idrissi, *J. Nano-Electron. Phys.* **15** No 1, 01026 (2023).
- S. Usha, P. Geetha, et al., *J. Nano-Electron. Phys.* **15** No 3, 03008 (2023).
- K. Jayanthi, A.M. Kalpana, et al., *J. Nano-Electron. Phys.* **15** No 3, 03022 (2023).
- R.M. Gomathi, M. Jeyabharathi, et al., *J. Nano-Electron. Phys.* **15** No 4, 04027 (2023).
- S. Al Perumal, M. Tabassum, N.M. Norwawi, G.A.N. Samy, *IEEE ICCSCE*, 70 (2018).
- I. Shammugam, G.N. Samy, P. Magalingam, N. Maarop, S. Perumal, B. Shanmugam, *Indonesian Journal of Electrical Engineering and Computer Science* **21** No 3, 1820 (2021).

Y-подібні патчі масивної MIMO-антени для вимірювання продуктивності при застосуванні 6GKumutha Duraisamy¹, P. Geetha², P. Gobi³, K. Arun¹, P. Latha⁴, Manjunathan Alagarsamy⁵¹ Department of CSE, Jeppiaar Institute of Technology, Kunnam, Sriperumudur, 631604 Chennai, India² Department of Electronics and Communication Engineering, Karpaga Vinayaga College of Engineering and Technology, 603308 Chennai, India³ Department of ECE, Jeppiaar Institute of Technology, Kunnam, Sriperumudur, 631604 Chennai, India⁴ Department of IT, Panimalar Engineering College, Chennai, India⁵ Department of ECE, K. Ramakrishnan College of Technology, Trichy, India

В сучасну епоху п'яте покоління (5G) визначає затримку на рівні 1 мс з високою швидкістю передачі даних для мереж мобільного зв'язку. Під час дослідження використання мереж 5G було виявлено вищий рівень енергоефективності та збільшення використання спектру в зоні покриття сигналу масивної антени 2-2 MIMO (Multiple Input and Multiple Output). Тому було представлено шосте покоління (6G), яке підтримуватиме масивну антену 2-2 MIMO у 10 разів краще, ніж 5G у системі мобільного зв'язку. 6G забезпечує 1 мкс з меншим споживанням енергії завдяки ефективності та однаковій частоті в конструкції масивної антени 2-2 MIMO. У мережах бездротового зв'язку також пропонується протокол, такий як Message Queuing Telemetry Transport (MQTT), для ефективного використання пропускну здатності та уникнення затримок під час передачі високошвидкісних даних для кількох користувачів. MQTT допомагає позбутися проблем безпеки під час кількох передач у системі масивної MIMO. Масивна антена 2-2 MIMO розроблена для частоти 10 ГГц для зменшення міжсимвольної інтерференції (ISI), що забезпечує ефективність 88 %. Y-подібні ділянки змодельовані з радіусом 8,5 мм у верхньому шарі для двох елементів. Розмір заземлення 8,5 мм × 65 мм × 2 мм забезпечують ефективність роботи. Запропонована система використовувала робочу частоту від 2,7 до 15,8 ГГц зі втратами на відбиття 15 дБ та ізоляцією 12 дБ для протоколу MQTT з масивною антеною MIMO. Високочастотний симулятор (HFSS) забезпечує відносну діелектричну проникність 2,7, ізоляцію 13 дБ та спрямованість 5. Також досягнуто коефіцієнта посилення 6,7 дБ з ефективністю 88 % порівняно зі звичайним методом.

Ключові слова: 6G, Масивний 2-2 MIMO, HFSS, MQTT, ISI, Мобільний зв'язок.